

Dynamic Remnant Vortices in Superfluid $^3\text{He-B}$

R. E. Solntsev^y, R. de Graaf^y, V. B. Eltsov^{yz}, R. Hanninen^y,
and M. Krusius^y

^y Low Temperature Laboratory, Helsinki University of Technology, Finland

^z Kapitza Institute for Physical Problems, Kosygina 2, 119334 Moscow, Russia

We investigate the decay of vortices in a rotating cylindrical sample, after rotation has been stopped. With decreasing temperature vortex annihilation slows down, as the damping in vortex motion, the mutual friction dissipation Γ , decreases exponentially. Remnant vortices then survive for increasingly long periods, while they move towards annihilation in zero applied flow. If rotation is reapplied, the remnants evolve to rectilinear vortices. By counting these lines, we measure in the regime $\Gamma \ll 1$ the number of remnants as a function of temperature T and the preceding waiting period t at zero applied flow. At lower temperatures, when $\Gamma \approx 0.4$, the lifetime of the last few remnants becomes hours. When flow is reapplied in this regime, an expanding remnant may become unstable and create a new vortex. Here we measure the onset temperature of turbulence T_{on} as a function of t and the applied flow velocity $v = v_n - v_s$.

PACS numbers: 67.40.Vs, 47.32.Cc.

In superfluid $^3\text{He-B}$ the length scale of the vortex core radius is the superfluid coherence length $\xi(T) = \xi(0)(1 - T/T_c)^{1/2}$, with $\xi(0) = 12-65 \text{ nm}$ for pressures $P = 34-0 \text{ bar}$. Apparently this is large enough compared to the typical surface roughness of our fused quartz sample cylinder that it has not been possible to measure surface pinning or friction. A sensitive test is to check for vortex formation when flow is reapplied, to find out whether remnant vortices have remained pinned at surface traps for indefinitely long waiting periods t in zero applied flow. If t is long enough, all previous vortices have annihilated, unless they become permanently pinned. At millikelvin temperatures the energy barriers associated with such pinning traps are typically large compared to thermal energies and once loaded, a trap remains occupied as long as the flow velocity v is kept at sufficiently low level. To release a remnant from the trap, the required applied flow velocity

Corresponding author: email rom an@boo.jut.

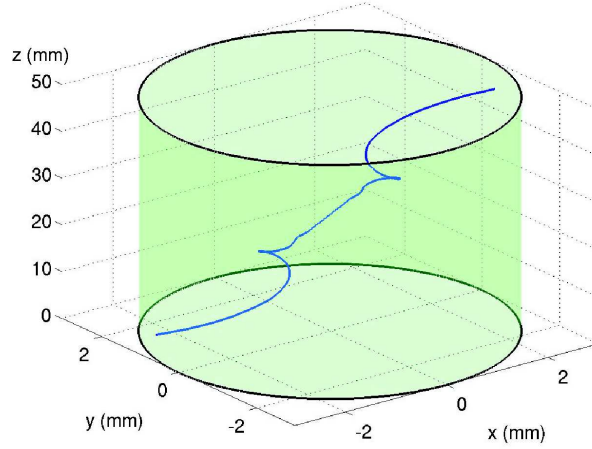


Fig. 1. A single remnant vortex in an ideal sample cylinder at zero applied flow in $^3\text{He-B}$ at $0.40 T_c$ and 29 bar. Both ends of the vortex move slowly in spiral motion around the cylindrical wall in the image flow field created by the vortex itself. This snapshot shows its configuration after 1.3 h of motion towards total annihilation which takes 2.3 h. The vortex was initially straight but tilted, with its ends at $(-1, 0, 0)$ and $(1, 0, 50)$ on the two flat end plates of the container, which is 50 mm long and 3 mm in radius.

is $v_c = 0.8 = (2/r_c)$, if the remnant is modeled as a half circle of radius r_c attached at both ends to the cylindrical wall.¹

The measurement is straightforward, but it involves three complications: (i) Remnants can exist on different length scales. The length scale determines the flow velocity at which a particular remnant is initiated out of the pinning trap. (ii) In the presence of only a few isolated pinning traps remanence has stochastic nature since during random annihilation a particular pinning site may or may not become loaded with a remnant. (iii) The dynamical behavior of vortices changes with temperature because of the exponentially temperature dependent mutual friction dissipation $(T; P)$.² At high temperatures vortex motion is rapid, like in a typical superconductor. When rotation is suddenly stopped from an equilibrium vortex state at $(t = 0)$, the decay of rectilinear vortices is of the form $N(t) / (1 + t\tau)^{-1}$, with a decay time $\tau = [2 \cdot \eta(0)]^{-1}$. In contrast, at low temperatures the motion of an isolated vortex at zero applied flow becomes sluggish, as known from $^4\text{He-II}$. Below $0.5 T_c$ the motion of the last vortex towards total annihilation may require hours. An example of a dynamic remnant from numerical calculations⁴ is shown in Fig. 1. In isothermal conditions it then becomes experimentally difficult to distinguish between pinned and dynamic remnants.

Remnant vortices in $^3\text{He-B}$

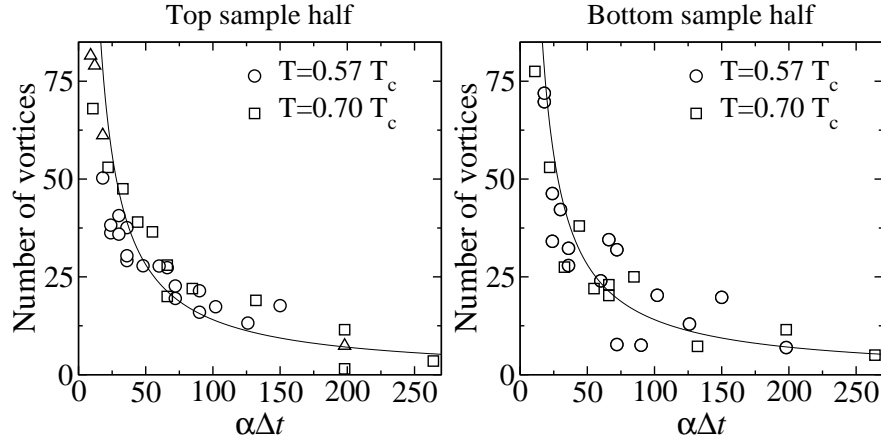


Fig. 2. Number of remnant vortices N as a function of the waiting period t at zero rotation. The results for the A-phase separated top and bottom sample sections can both be fitted with $N(t) = 1.4 T_c^3 \Theta(t)$ [with t in seconds], i.e. the remnants annihilate monotonically with increasing t , as expected for mutual friction controlled dynamic remanence. The data are for $\Omega = 0.9 \text{ rad/s}$ at $0.57 T_c$ with $\alpha = 0.60$ and $0.7 T_c$ with $\alpha = 1.1$.

Experimental setup: We measure with non-invasive NMR techniques the number of vortex lines at 29.0 bar pressure in a sample cylinder with radius $R = 3 \text{ mm}$ and length $L = 110 \text{ mm}$. NMR detection coils are located around both ends of the sample.⁵ The sample can also be studied in a different configuration: By sweeping up a magnetic barrier field $H_b > H_{AB}(T; P)$ over the central section of the long sample, a layer of $^3\text{He-A}$ divides the cylinder in two $^3\text{He-B}$ samples with lengths $L_t = 44 \text{ mm}$ for the top and $L_b = 54 \text{ mm}$ for the bottom section (at $0.5 T_c$). The A phase layer acts as a barrier⁶ for vortices such that the two B-phase sections can be studied independently. By rotating the sample cylinder around its symmetry axis with angular velocity Ω , the maximum flow velocity is reached at the cylindrical wall, $v(N) = \Omega R$ ($N = 2 R \lambda$), where N is the number of rectilinear vortex lines in a central vortex cluster. N is determined by comparing the NMR line shape to one measured with a known number of vortices.

Measuring procedure: We start from a state with large N at $\Omega = 1.7 \text{ rad/s}$ which is decelerated at 0.02 rad/s^2 to zero rotation and kept there for a waiting period t . Rotation is then increased (in the same direction) at 0.01 rad/s^2 to Ω_f where it is kept constant. The NMR line shape measured at Ω_f , after all transients have decayed, is compared to a calibration with a known number of rectilinear vortices.⁵ This gives N in the final state at Ω_f . Our measurements are performed in the temperature range where the superfluid equivalent⁵ of the Reynolds number $q^{-1}(T) = (1 - T/T_c)^2$ is of order

1. At temperatures above the vortex instability⁷ (when $(T;P) > 0.4$) we equate N with the number of remnants N at the end of the waiting period t . At lower temperatures (when $(T;P) < 0.4$) the vortex instability leads to the generation of new vortices and the number of vortices increases in applied flow. We then measure the onset temperature T_{on} of turbulence. In both cases a remnant which starts to evolve has to be above a minimum size. At $\Omega_f = 0.9 \text{ rad/s}$ the minimum radius is $r_c \approx 3 \text{ m}$. In comparison, the measured roughness of the quartz surface is typically $\approx 1 \text{ m}$. We also studied whether the rate of change of the rotation drive $j_l = d\Omega/dt$ influences the results for $N(t)$. No dependence was observed in our operating range $0.001 - 0.04 \text{ rad/s}^2$, when $t = 90 \text{ s}$.

Regime of constant vortex number: In Fig. 2 results are shown for higher temperatures where no new vortices are formed. When the waiting period t is a few seconds the number of remnants $N(t)$ is around 100 while when $t = 10 \text{ min}$ it has smoothly decayed to a few. The same decay $/ (t)^{-1}$ is measured independently for the top and bottom sample sections. These two smooth decays exclude large numbers of permanently pinned vortices in pinning configurations larger than the equivalent of $r_c \approx 3 \text{ m}$. From our extensive attempts⁸ to exclude remnants and to achieve vortex-free flow, we conclude that the decay of remnants is governed by t and T . Together they control the number, size, and configuration of remnants. To reach a vortex-free flow state at lower temperatures one has to extend t to longer and longer times. The final state of remanence with long life time seems to be one where only one remnant exists in each cross section of the cylinder. In a long cylinder many remnants can still be stacked after another in configurations like that in Fig. 1. As seen in Fig. 3, in the present cylinder it is possible to reach consistently vortex-free flow up to $\approx 1 \text{ rad/s}$ at temperatures down to $0.4 T_c$, applying a waiting period $t = 20 \text{ min}$. In comparison, by cooling from high temperatures in rotation, vortex-free flow at 1 rad/s can be maintained at least to below $0.2 T_c$.

Regime of vortex multiplication: In Fig. 3 we perform the previous measurement as a function of temperature at two values of t , namely 2 and 20 minutes. Here we plot on the vertical axis the probability to create new vortices. It turns out that once the vortex instability⁷ becomes possible, it almost inevitably leads to turbulence which then brings the sample in the equilibrium vortex state. Examples, where much less than the equilibrium number of vortices would be created, are rare and limited to the onset regime around T_{on} . New vortices are created when the curved remnants become unstable with respect to Kelvin wave formation in the the applied flow and interact with the cylindrical wall. The active vortices, which contribute to this process, are those with one or both ends on the cylindrical wall,

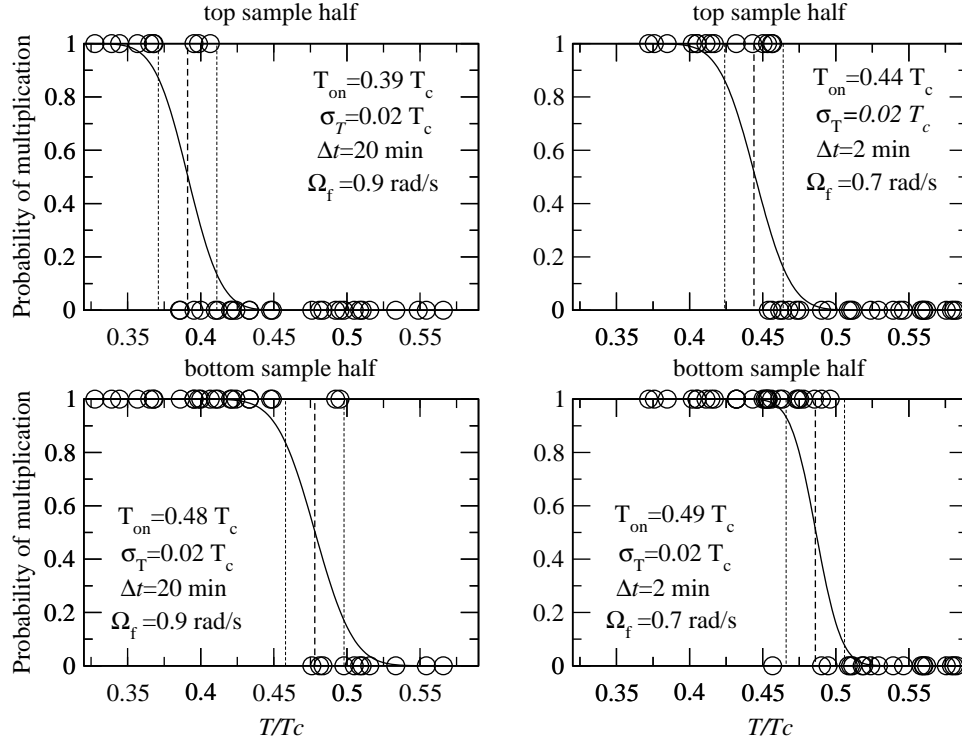


Fig. 3. Onset temperature T_{on} of turbulence, measured for A-phase separated top and bottom sample sections. The probability of finding the equilibrium vortex state at Ω_f is plotted as a function of temperature with 20 { 25 data points per panel. Two cases are compared: (a) $t = 20$ min, $\Omega_f = 0.9$ rad/s and (b) $t = 2$ min, $\Omega_f = 0.7$ rad/s. The two samples show different behavior: In the top T_{on} decreases with increasing t , as the number and size of remnants is reduced. The bottom sample is dominated by the ejection of vortex loops from the ori ce.

while rectilinear vortices in the center of the sample are stable. When the density of active vortices becomes sufficiently high somewhere at the cylindrical wall, such that loop interactions become important, then turbulence becomes possible. In this way turbulence can start even from a single curved vortex, although T_{on} depends on the number and size of initial seeds. In the top sample section T_{on} is lower for $t = 20$ min than for $t = 2$ min, since the number of remnants is reduced by an order of magnitude to only a few (if one uses the fit to the data in Fig.2), in spite of the fact that the latter case has been measured at a 30 % lower value of applied flow velocity. The distribution of the data in the onset regime can be fit with a normal distribution and a halfwidth $\sigma_T = 0.02 T_c$. There exists no single data point from

well above T_{on} which shows any large increase in vortex number (beyond our resolution of 10 vortices) or from well below T_{on} such that the final stable state would not be very close to the equilibrium vortex state. The bottom sample section displays a higher T_{on} with no clear dependence on Ω . We attribute this to the vortex instability in the orifices on the bottom of our sample cylinder. The comparatively low values of T_{on} in the top section suggest that the AB interface, rather than supporting remanence, acts to reduce it. At these lower temperatures the remanents are largely insensitive to the direction of rotation after the waiting period, since they are easily reoriented by the applied flow. With these interpretations all our results become consistent with dynamic remanents.

Consequences: In contrast to superfluid $^4\text{He-II}$, it appears that sufficiently smooth-walled containers can be found for $^3\text{He-B}$ in which vortices are not permanently pinned by surface roughness. The present measurements leave open the question about the magnitude of surface friction in a weak pinning model,³ but clearly vortex-free rotating flow can be achieved in an open cylinder with non-invasive measurements, i.e. without internal probes or other components which enhance pinning because of non-uniform geometry. This allows studies on vortices with new experimental approaches, such as the injection of seed vortices in applied flow. However, with decreasing temperature mutual friction dissipation diminishes and vortex annihilation becomes exceedingly slow. At the lowest temperatures the last dynamic remanents can only be removed by warming up to higher temperatures, to speed up annihilation. Using thermal cycling, relatively high-velocity stable vortex-free flow appears to be possible even in the zero temperature limit.

It is generally assumed that remnant vortices originate from surface pinning in $^4\text{He-II}$. However, since $\Omega = 0.1$ in most of the experimental temperature range of $^4\text{He-II}$, dynamic remanence has to be even more prevalent there than in $^3\text{He-B}$. With careful selection and preparation of the container walls one can suppress surface roughness below 1 nm , so that trapped remanents will remain immobile at $\Omega = 1\text{ rad/s}$. Within this range of flow the present considerations about dynamic remanents apply also for $^4\text{He-II}$.

REFERENCES

1. V.M.H. Ruutu et al., J. Low Temp. Phys. 107, 93 (1997).
2. T.D.C. Bevan et al., J. Low Temp. Phys. 109, 423 (1997).
3. M.K. Khusiis et al., Phys. Rev. B 47, 15113 (1993-II).
4. R. Hanninen, A. Mitani, and M. Tsubota, J. Low Temp. Phys., 138, 589 (2005).
5. A.P. Finne et al., J. Low Temp. Phys. 136, 249 (2004).
6. R. Blaauwgeers et al., Phys. Rev. Lett. 89, 155301 (2002).
7. A.P. Finne et al., Phys. Rev. Lett. 96, 85301 (2006).
8. R. de Graaf et al., submitted to these proceedings, J. Low Temp. Phys. (2007).